ELSEVIER

Journal of Power Sources 62 (1996) 59–66

JOURNAL OF POWER SOURCES

Synthesis of $LiNiO_2$ in air atmosphere: X-ray diffraction characterization and electrochemical investigation

R. Moshtev [a,*], P. Zlatilova [a], V. Manev [a], K. Tagawa [b]

[a] *Central Laboratory of Electrochemical Power Sources, Bulgarian Academy of Sciences, Sofia 1113, Bulgaria*

[b] *Hohsen Corporation, R&D Department, Osaka 542, Japan*

Received 22 September 1995; revised 26 January 1996; accepted 9 February 1996

Abstract

The synthesis of $LiNiO_2$ in air is studied by means of X-ray diffraction (XRD) characterization using a new fast method based on the splitting of the (108) and (110) peaks and the depth of the minimum between these peaks. From the evolution of these XRD parameters during the heat treatment of the starting mixture of LiOH and NiO the optimum synthesis time is determined, where the separation angle has a maximum, implying a good stoichiometry and low cation disorder; the minimum between the peak is deepest, indicating a better crystallinity. Selected samples of $LiNiO_2$ were cycled as cathodes in laboratory-coin cells between constant charge and discharge end voltages at a constant current. It is found that the capacity decay rate is related to the phase transitions occurring during cycling. This rate is dependent on the minimum lithium content x in $Li_xNi_{2-x}O_2$ at the end of charge. As the cycling proceeds x_{min} increases despite that the end charge voltage is kept constant, whereby the capacity decay rate diminishes.

Keywords: Lithium nickel oxide; Lithium cells; Cycling performance; Cycling behaviour

1. Introduction

The synthesis in oxygen atmosphere of almost stoichiometric $Li_xNi_{2-x}O_2$ with $0.97 \leq x \leq 0.99$ is comparatively easy, since the higher pO_2 suppresses the thermal decomposition of the product whereby the stoichiometry of the phase remains high. The synthesis in air, however, especially under plant conditions offers some technological advantages which cannot be neglected. This explains the interest of many authors in studying the synthesis of $LiNiO_2$ without the use of pure oxygen.

In 1989 scientists of the French battery company SAFT developed and patented such a method starting from $LiOH \cdot H_2O$ and NiO [1]. The stoichiometry claimed in this patent, $x = 0.93$, was not satisfactory, so that several improved methods were elaborated. The methods applied and the stoichiometry achieved so far are summarized in Table 1 based on data from the open literature.

The X-ray diffraction (XRD) characterization of the $LiNiO_2$ phase is a very important tool in following the high temperature synthesis. The most precise XRD data can be obtained by the Rietveld profile analysis. In view of the complexity and longer XRD apparatus time the Rietveld method is not very suitable for optimization studies. In such cases it is more appropriate to use simpler and faster XRD techniques yielding not exact but sufficiently reliable data.

Morales et al. [8] were the first researchers to correlate semi-quantitatively the integrated intensity ratio of the (003) and (104) reflexes with the lithium content in samples with $x < 0.9$. The ratio was later used by Ohzuku et al. [5] as a qualitative criterion for the stoichiometry of samples with $x \geq 0.96$. Dahn et al. [2] derived theoretically and confirmed experimentally the relationship between x and the integrated intensity ratio between the (102) + (006) and (101) reflexes, which they claim to be more reliable, because of the proximity of the peaks involved in this ratio. The splitting of the (108) (110) peaks is mentioned by Ohzuku et al. [5] as a possible qualitative criterion for the stoichiometry of the phase.

In the XRD patterns obtained during the synthesis of $LiNiO_2$ in previous works [5,6] it can be seen that as the synthesis advances and the stoichiometry of the sample increases the splitting between the (108) and (110) peaks grows and the minimum between them deepens. The narrow scale of these X-ray profiles, however, does not allow any quantitative evaluation of these parameters. In a recent short communication [9] we have tried to correlate the angle separation between these peaks obtained by computer-acquired

* Corresponding author.

PII S0378-7753(96)02402-0

Table 1
Synthesis conditions of $LiNiO_2$ in air atmosphere

No.	Refs.	Starting materials	Li/Ni ratio	Temperature (°C)	Time (h)	x_{max}
1	[2]	$LiOH + Ni(OH)_2$	1.1	600	5	0.96
2	[3]	$LiOH + Ni(OH)_2$	1.0	700	2	0.99
3	[4]	$LiOH + Ni(OH)_2$	1.1	650	21	0.99
4	[5]	$LiOH + Ni(OH)_2$	1.0	800	24	
5	[6]	$LiOH + Ni(OH)_2$		700	5	0.95
6	[7]	$LiOH + Ni(OH)_2$		700		0.97

data of $\Delta 2\theta$ versus the intensity and the stoichiometric number x determined by chemical analysis, but the data points were rather scattered.

In this paper, an attempt is made to correlate quantitatively the angle separation with the stoichiometric number of a series of $LiNiO_2$ samples synthesized in air as well as to evaluate qualitatively the crystallinity of the samples by the depth of the minimum between the peaks. These XRD parameters are employed in the optimization of the synthesis of $LiNiO_2$ in air. Selected samples with optimum XRD parameters are characterized electrochemically in cycling tests.

2. Experimental

2.1. XRD characterization

The development of the present fast XRD method for the characterization of $Li_xNi_{2-x}O_2$ samples is based on the linear relationship between the c/a ratio and the stoichiometric number x, recently derived by Li and Reimers [3] in the range $0.62 \leq x \leq 1.0$. Our first task was to determine the accuracy of the c/a ratio obtained on the basis of the two closely positioned high angle peaks of the (108) and (110) planes. For this purpose the c/a ratios of a series of samples were assessed by two methods:

(i) By calculation the c- and a-parameters from the expression for the hexagonal lattice

$$\sin^2\theta = A(h^2 + k^2 + hk) + Cl^2 \quad (1)$$

where $A = \lambda^2/3a^2$ and $C = \lambda^2/4c^2$ on the basis of the (108) and (110) peak positions recorded on the XRD diagram at a rate of 0.5° (2θ) per min and a paper propagation rate of 4 cm/min between 63.5 and 65.5°. This value is denoted as $(\bar{c}/\bar{a})_2$.

(ii) By accurate determination of the lattice parameters by the least-squares method on the basis of the peak angles of the nine strongest reflections: (003), (101), (102), (104), (105), (107), (108), (110) and (113). The peak positions in this case were determined by a computer program, scanning 80 points at intervals of $2\theta = 0.02°$ for 2 s each around the peak maximum. This value we denote here as $(\bar{c}/\bar{a})_9$.

All XRD measurements were performed with Cu Kα irradiation on a Philips powder diffractometer, APD-15 provided with a P-830-010 computer.

The minimum between the (108) and (110) peaks was characterized by the arbitrary ratio $R_m = H_{min}/H_{(108)}$, where H_{min} is the height at the minimum and $H_{(108)}$ the height of the (108) peak.

2.2. Synthesis

Samples of $LiNiO_2$ were synthesized by heating appropriate amounts of $LiOH \cdot H_2O$ and NiO mixed by grinding in a mortar. $LiOH \cdot H_2O$ was used as supplied (Fluka), while NiO was prepared by gradual heating of nickel(II) hydroxycarbonate $\cdot H_2O$ up to 420 °C. The starting materials were analysed chemically for lithium and nickel, respectively, in order to determine the Li/Ni ratio in the reaction mixture. The specific surface area (BET) of the NiO powder amounted to 34 m^2/g. The synthesis was carried out in alumina or nickel crucibles in a tube oven whose temperature could be controlled within ±5 °C. The mixture was heated preliminary at 650 °C for 2 h and after grinding it was heat-treated at a constant temperature between 650 and 800 °C during 2 to 24 h under air flow at a rate of about 3 l/h under intermittent grinding. In some cases, an oxygen flow was used for the sake of comparison. Both gases were purified from water vapour and CO_2 in appropriate columns with molecular sieves and KOH pellets.

2.3. Electrochemical testing

Positive electrodes were prepared by mixing selected samples of $LiNiO_2$ with 20% of teflonized acetylene black and pressing on aluminium foil discs (diameter: 15 mm). They were cycled at constant current, $I = C/5$, in laboratory steel coin cells provided with a lithium reference electrode and lithium counter-electrodes. The cells simulate closely the conditions in a commercial coin cell, i.e. with limited electrolyte volume, tightly packed electrodes separated by a sheet of Whatman glass paper and a sheet of Celgard 2502. The electrolyte solution was 1 M $LiClO_4$ in a 1:1 mixture of propylene carbonate (PC) and ethylene carbonate (EC) with a water content less than 30 ppm.

3. Results

3.1. XRD measurements

The results of the (c/a) parallel measurement of seven samples with different stoichiometry by the fast and accurate

methods are displayed in Fig. 1. The straight line marks the complete agreement between the two (c/a) values. The maximum experimental deviation is 0.0014 while the mean standard deviation is 4.6×10^{-4}. This result renders possible the use of the fast method for the assessment of the $(\bar{c}/\bar{a})$ ratio and consequently for the stoichiometric number x.

The relationship between $\Delta2\theta$ and $(\bar{c}/\bar{a})_2$ calculated by Eq. (1) is presented in Fig. 2. In the experimentally significant range $0.24°\leq\Delta2\theta\leq0.34°$ each of the $(\bar{c}/\bar{a})_2$ values was calculated at several different values of the peak angle 2θ of the (108) reflex in the range 64.34° to 64.50° at a constant angle separation. The linear plot in Fig. 2 with points independent of the variations in the peak positions reveals that the angle separation could be used for the reliable assessment of the $(\bar{c}/\bar{a})$ ratio and consequently for the evaluation of the stoichiometric number x on the basis of the data recently reported by several authors [3,4,11]. It shows also that the eventual errors in the exact determination of the peak positions will have no impact on the $(\bar{c}/\bar{a})$ ratio. It should be pointed our that the independence of $(\bar{c}/\bar{a})_2$ from the variations of the peak angles holds true only for the low values of $\Delta2\theta$ observed experimentally. At higher $\Delta2\theta$ values, e.g. $>0.8°$, the variation of the $(\bar{c}/\bar{a})_2$ ratio with the peak positions is considerable.

Fig. 3 presents the plot of the stoichiometry number x in $Li_xNi_{2-x}O_2$ versus c/a ratio with the data of Reimers et al. [4] and Kanno et al. [11] determined by Rietveld profile refinement. The x data of Kanno et al. [11] refer to the occupancy by lithium of the 3b layer, which explains the large deviation of their value at x close to unity. The upper abscissa in Fig. 3 gives the $\Delta2\theta$ values derived from the c/a versus $\Delta2\theta$ plot in Fig. 2. The straight line is the least-square fit of the data. Since the accuracy of the $\Delta2\theta$ determination is $\pm0.005°$ the accuracy of x obtained from the plot in Fig. 3 is ±0.01, which is sufficient for the purpose of the optimization task.

The XRD patterns of the (108) and (110) peaks in Fig. 4 demonstrate the evolution of a typical synthesis process in

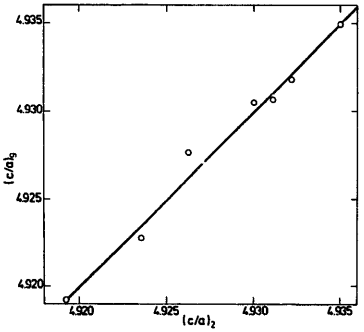

Fig. 1. Correlation between $\bar{c}/\bar{a}$ ratios obtained by the approximate method, $(\bar{c}/\bar{a})_2$, and by the least-squares method from nine peaks, $(\bar{c}/\bar{a})_9$.

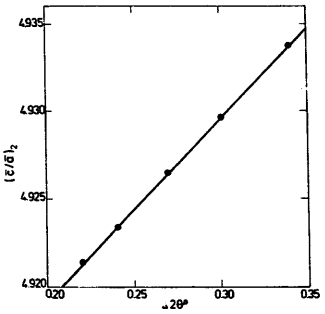

Fig. 2. Relationship between the peak separation, $\Delta2\theta$, and the $(\bar{c}/\bar{a})_2$ values estimated at different peak angles of (108) varied between 64.34° to 64.50°.

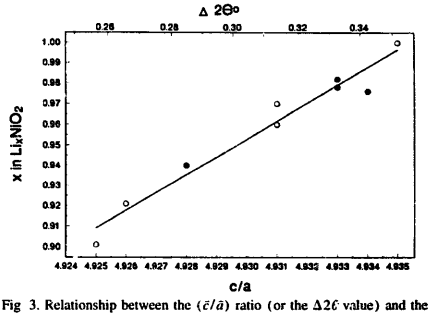

Fig 3. Relationship between the $(\bar{c}/\bar{a})$ ratio (or the $\Delta2\theta$ value) and the stoichiometry number x in $Li_xNi_{2-x}O_2$ from literature data: (○) Ref. [4], and (●) Ref. [11].

air of an $Li_xNi_{2-x}O_2$ sample at 750 °C with a 2% lithium excess in the starting mixture. In curve (a) recorded after the preliminary heat treatment for 2 h at 650 °C no splitting is observed revealing the absence of the hexagonal phase. After 2 h of heating at 750 °C the splitting appears (curve (b)) with $\Delta2\theta=0.27°$, but the minimum between the peaks is rather shallow, corresponding to a high value of $R_m=0.92$. After 8 h at 750 °C the angle separation reaches a maximum value of 0.32° and due to the higher and sharper peaks the minimum is much deeper with $R_m=0.68$ (curve (c)). This sharpness is exhibited also by the appearance of the shoulder at about 64.84° probably corresponding to the reflex of the (110) peak due to the separation of the α_2 doublet. The further thermal treatment at 750 °C up to 14 h (curve (d)) brings about a considerable reduction of the angle separation down to 0.26° and of the peaks sharpness, as revealed by the increased value of $R_m=0.72$.

The evolution of the angle separation and of the R_m ratio during this synthesis is more clearly displayed in Fig. 5. The results presented in this figure allow us to distinguish the different stages in the synthesis process of $LiNiO_2$ in air:

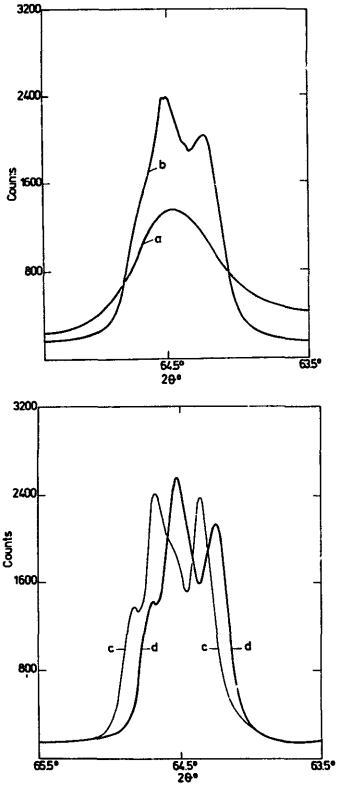

Fig. 4. XRD patterns of the (108) (110) peaks recorded during the synthesis of $Li_xNi_{2-x}O_2$ at increasing time of the thermal treatment in air atmosphere: (a) 2 h at 650 °C; (b) 2 h at 750 °C; (c) 8 h at 750 °C, and (d) 14 h at 750 °C.

(i) as lithium penetrates in the crystal lattice of NiO the cubic $Li_xNi_{2-x}O_2$ phase is first formed with $x < 0.62$, whereby no splitting of the peaks is observed (curve (a));

(ii) when more and more lithium atoms are inserted into the cubic phase the latter is transformed into the hexagonal one but with $\Delta 2\theta = 0.27°$ corresponding to $x = 0.93$ and a shallow minimum characteristic for small crystal domains (curve (b));

(iii) after 8 h at 750 °C the maximum of $\Delta 2\theta = 0.32°$ is reached (curve (c)) corresponding to $(\bar{c}/\bar{a}) = 4.932$ or $x = 0.97$ with a deep minimum, $R_m = 0.68$, revealing the presence of larger crystal domains with a good stoichiometry and this could be assumed as the optimum synthesis time, τ_{op}. It was shown earlier in the case of $LiNiO_2$ synthesized in oxygen [9,10] that samples with $x = 0.97$ display a fairly good electrochemical performance;

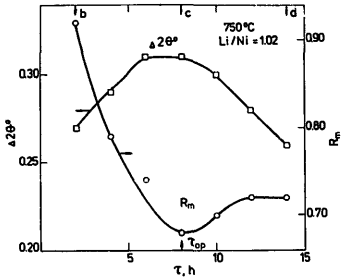

Fig. 5. Evolution of the peak separation $\Delta 2\theta$ and the R_m ratio during the synthesis of $Li_xNi_{2-x}O_2$ in air at 750 °C.

(iv) it can be supposed that at the optimum synthesis time all the available lithium has been consumed so that the synthesis reaction

$$0.5Li_2O + NiO + 0.25O_2 = LiNiO_2 \quad (2)$$

practically cannot proceed anymore. If the heat treatment continues after that, due to the low pO_2 in the air, conditions will be favourable for the decomposition reaction

$$(1+x)LiNi^{3+}O_2 \rightarrow Li_{1-2x}Ni_x^{2+}Ni^{3+}O_2 + 1.5xLi_2O + x/4O_2 \quad (3)$$

to proceed. The differential gravimetric analysis (DGA) data of Kanno et al. [11] reveal that the decomposition of $LiNiO_2$ in air proceeds noticeably at temperatures above 700 °C. On the other hand, our own results of synthesis at 800 °C showed that reaction (3) cannot be suppressed by increasing the lithium excess in the reaction mixture. Therefore, it can be assumed that the decomposition of $LiNiO_2$ in air is controlled by the reduction of Ni^{3+} to Ni^{2+} and is accompanied by extraction of Li_2O from the phase. When the lithium content at the surface of the hexagonal crystallites falls down below $x = 0.62$ the cubic phase will appear with smaller crystallites at first. These changes in the product are recorded in curve (d) with a smaller angle separation and a higher R_m value in comparison with those in curve (c).

From a practical point of view plots as those in Fig. 5 could be conveniently used in determining the optimum synthesis time τ_{op} under various conditions. Since the recording of the XRD patterns as those in Fig. 4 takes only 5 to 6 min it is possible to control very efficiently the quality of the product during synthesis.

3.2. *Effect of synthesis temperature on optimum XRD parameters*

Several series of syntheses were performed at each of the following temperatures: 650, 700, 750 and 800 °C. At

Table 2
Effect of the synthesis temperature on the mean XRD parameters at the optimum synthesis time

Synthesis conditions			Mean XRD parameters		
t (°C)	τ_{op} (h)	Li excess (%)	$\Delta 2\theta$	R_m	R_c
650	25±6	2	0.28	0.85	0.33±0.02
700	9±3	2	0.29	0.83	0.35±0.02
750	6±2	2	0.32	0.74	0.45±0.02
800	2±0.5	5	0.29	0.81	0.36±0.02

600 °C we could not observe any splitting of the (108) and (110) peaks even after 24 h. The XRD data of the samples recorded during the syntheses were plotted as a function of the time of heat treatment as in Fig. 5, whereby the optimum synthesis time was established. Since, as it will be shown in the following, the electrochemical performance of the cathodes with $LiNiO_2$ depends both on the stoichiometry and on the crystallinity of the sample we introduced the arbitrary criterion $R_c = \Delta 2\theta / R_m$, which accounts for both factors. Table 2 summarizes the results of these experiments.

The data in Table 2 reveal that the synthesis time for optimum XRD parameters should be strongly reduced with the increase in synthesis temperature in order to prevent the decomposition of the product at temperatures above 700 °C in air atmosphere. At 800 °C, this rate is so high that the maximum R_c value attained is considerably lower than that obtained at 750 °C. At temperatures below 750 °C the decomposition rate is low but the synthesis time is much longer whereby the decomposition Eq. (3) can proceed sufficiently as to reduce the stoichiometry of the product.

On the other hand, the samples synthesized at 750 °C for 24 h in oxygen with only a 1% lithium excess exhibited the maximum angle separation of 0.34° corresponding to an almost perfect stoichiometry, $x = 0.99$, this leading to a high value of $R_c = 0.47$. This result shows clearly that the decomposition Eq. (3) is strongly suppressed by the stabilization of the Ni^{3+} ions in the crystal lattice of $LiNiO_2$ at higher oxygen concentrations and not by a larger excess of lithium in the reaction mixture.

3.3. Electrochemical performance

The voltage profiles during charge and discharge of the $LiNiO_2$ cathodes in the first cycles at low and moderate rates exhibit four well-expressed plateaus which are characteristic for a material with good stoichiometry and crystallinity. The voltage profiles of cathodes prepared with $LiNiO_2$ samples synthesized in air with $x = 0.95 - 0.97$ in the present investigation revealed well-expressed plateaus at 3.65, 4.00 and 4.18 V and a less visible one at about 3.75 V. Practically the same plateaus were observed previously with $LiNiO_2$ samples obtained in oxygen [5,10,14] and in air [7].

The low coulombic efficiency (*CE*) in the first cycle, CE_1, of about 75–77% is related to the capacity loss inherent in $LiNiO_2$. In the next 2 to 5 cycles *CE* increases to reach 97.5 to 99.5%. It was earlier established in our experiments that cycling at *CE* lower than 97% brings about a much faster capacity decay. The results of such cycling tests were discarded since the purpose of our experiments was to reveal the relationship between the cycling behaviour of the material and the changes in its crystal structure, eliminating as far as possible the effect of all other 'secondary' factors on the capacity decay. The negative effects of poor contacts and dendritic shorts, as well as of possible exfoliation of the cathode mix from the aluminium substrate were suppressed by the application of a moderate pressure of about 3 kg/cm^2 on the electrodes. Further, a *CE* better than 97.5% was achieved by using high purity electrolyte materials and in some cases a lower content of acetylene black in the cathode mix. This was very important in view of the fact that our laboratory cells simulated the conditions of real cells where the electrolyte volume is limited only in the pores of the cathode and in the separator.

An attempt was made to correlate the cycling performance of the cathodes with the XRD parameters of the samples. As it will be seen in the results presented in Fig. 7 the discharge capacity of the cathodes is stabilized after the 20th cycle. Hence, as a criterion for the cycling performance in this experiment we assumed the discharge capacity at the 20th cycle which was obtained after cycling between 2.60 and 4.20 V at a *C*/5 rate at room temperature. The results in Table 3 reveal that the value of the discharge capacity cannot be well correlated with only one of the two XRD parameters either $\Delta 2\theta$ or R_m. As seen in Fig. 6, however, a fairly good correlation is obtained between C_{20} and the arbitrary ratio $R_c = \Delta 2\theta / R_m$, which accounts for both the stoichiometry and the crystallinity of the sample.

As far as the effect of the crystallinity is concerned the recent results of Xie et al. [12] showed that the capacity decay rate of $LiNiO_2$ cathodes with $x = 0.973$, synthesized in oxygen, strongly increases as their specific surface area (BET) grows from 0.8 to 1.6 m^2/g, i.e. with a decrease in crystallinity.

The strong effect of the end charge voltage U_{max} on the cycle life of the $LiNiO_2$ cathodes is well established [5,7].

Table 3
Dependence of C_{20} on XRD parameters

Sample no.	$\Delta 2\theta°$	R_m	$R_c = \Delta 2\theta°/R_m$	C_{20} (mAh/g)
1	0.24	0.88	0.27	95
2	0.25	0.70	0.36	115
3	0.30	0.78	0.38	130
4	0.31	0.73	0.42	142
5	0.26	0.60	0.43	140
6	0.30	0.66	0.45	140
7	0.32	0.66	0.48	143
8	0.32	0.63	0.51	160

Note: Sample No. 8 was synthesized in oxygen.

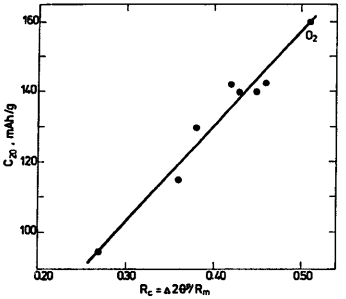

Fig. 6. Correlation between the $R_c = \Delta 2\theta / R_m$ ratio and the capacity of the cathodes at the 20th cycle; $U_{max} = 4.20$ V, $U_{min} = 2.60$ V, $I = C/5$.

Having in mind that the value of U_{max} determines the lithium content x_{min} at the end of the charge in $Li_xNi_{2-x}O_2$, and consequently, as shown in Refs. [5,14], the phase stability regions and the phase transitions occurring in the compound, it was of interest to examine the cycling behaviour of the cathode with respect to the phases appearing at the end of the charge.

For this purpose we plotted the value of x_{min} attained at the end of the charge in the cycling test, corrected by the coulombic efficiency, as well as the value of x_{min} reached at the end of the discharge as a function of the cycle numbers, n. Fig. 7 presents three pairs of such plots obtained from the charge/discharge capacities of Li_xNiO_2 cathodes from one and the same sample with $x = 0.97$ synthesized in air, cycled to three different U_{max}'s at a $C/5$ rate. The phase stability and the phase transition regions as determined by Ohzuku et al. [5] are also shown in the figure [5,14].

As a quantitative characteristic for the capacity decay rate we use in the following the DR constant estimated by the logarithmic law for the capacity decay of intercalation compounds proposed by Yamaki and Tobishima [13]

$$\log CS = \log(1 - DR) = \log(C_n/C_m)/(n-m) \qquad (4)$$

where CS is the cycling stability constant, C_n and C_m are the capacities at the nth and the mth cycle (with $n \gg m$) and $DR = (1 - CS)$ is the decay rate constant introduced here as a more explicit characteristic of the capacity decay rate.

Fig. 7 compares the dependencies of x_{min} and x_{max} versus n of three cathodes charged to 4.13, 4.20 and 4.28 V corresponding, respectively, to x_{min} of 0.31, 0.17 and 0.12 in the first charge. The value of x_{max} at the end of the discharge of the three cathodes is one and the same, 0.76, reflecting the same value of the end discharge voltage, 2.60 V, in the upper part of the stability range of phase R_1. This value of x_{max} is maintained constant during the entire cycling experiment and determines the inherent capacity loss of $LiNiO_2$ in the first cycle of 66 mAh/g.

For the cathode charged to $x_{min} = 0.30$ (Fig. 7(a)) the reversible transition at the end of the charge $M \leftrightarrow R_1'$ determines the extremely low decay rate constant between the 20th and 50th cycle, $DR_2 \leq 10^{-4}$ the exact value of which could be estimated from the data of a much longer cycling test. This approximate DR_2 value predicts a very long cycle life of the cathode. Using Eq. (4) it was found that it could yield about 1900 cycles before its capacity fell to 100 mAh/g, provided that the DR_2 value remains constant and the effect of the 'secondary' factors is negligible.

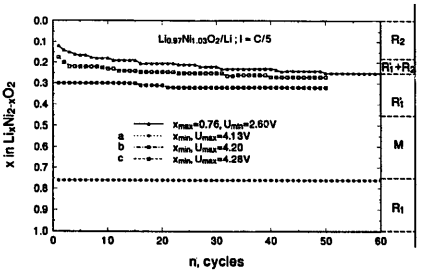

Fig. 7. Evolution of x_{min} and x_{max} of three $Li_{0.97}NiO_2$ cathodes with n charged to U_{max}: (a) 4.13 V ($x_{min} = 0.31$); (b) 4.20 V ($x_{min} = 0.18$), and (c) 4.28 V ($x_{min} = 0.12$). Discharge to 2.60 V for the three cathodes, rate of charge and discharge: $C/5$, room temperature. R1: the hexagonal $R\bar{3}m$ phase with $\bar{c} = 14.20$–14.24 Å; M: the monoclinic $C2/m$ phase with $\bar{c} = 14.30$–14.44 Å; R_1': the hexagonal $R\bar{3}m$ phase with $\bar{c} = 14.44$–14.43 Å, and R_2: the hexagonal $R\bar{3}m$ phase of NiO_2 with $\bar{c} = 13.52$–13.43 Å [5,14].

The evolution of x_{min} with n of the cathode cycled to 4.20 V, i.e. to $x_{min} = 0.17$ in the first cycle, is presented by curve (b) in Fig. 7. Under this condition the phase R_2 appears at the end of the first 17 charges. As the cycling proceeds x_{min} grows reaching 0.26 after the 17th cycle, where the irreversible phase R_2 does not appear anymore.

Consequently the rate constant in the first 20 cycles, $DR_1 = 2.85 \times 10^{-3}$ falls to 1.7×10^{-3} in the next 30 cycles. Using the latter value it was found by Eq. (4) that this cathode could by cycled 220 times before reaching the minimum capacity of 100 mAh/g.

Curve (c) in Fig. 7 displays the evolution of x_{min} of the cathode charged to 4.28 V or $x_{min} = 0.12$ in the first cycle, i.e. in the region where the R_2 phase is predominant. This explains the partially irreversible behaviour of the cathode in the first 20 cycles where $DR_1 = 5.05 \times 10^{-3}$. After the 10th cycle the value of x_{min} rises to 0.19, i.e. in the two phase region ($R_1' + R_2$), whereby the irreversibility is noticeably lowered. It is only after the 50th cycle, however, that x_{min} attains the value of 0.25, whereafter the partially irreversible phase R_2 appears no more. Consequently, no capacity decay is observed in the next ten cycles. On the basis of $DR_2 = 2.05 \times 10^{-3}$ estimated between the 20th and the 60th cycle it was found that this cathode could be cycled 224 times before reaching the minimum capacity of 100 mAh/g. The same cycle life as that of the previous cathode is to be expected, but the accumulated capacity will be evidently greater.

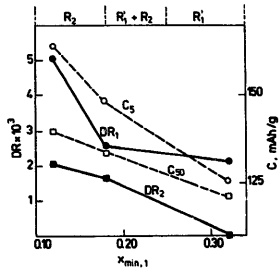

Fig. 8. Dependence of the decay rate constant DR_1 and DR_2 and the capacities C_5 and C_{50} on the value of x_{min} during the first cycle.

The steep capacity decay of the cathode cycled to 4.28 V (Fig. 7(c)) is obviously determined by the faster increase in x_{min}, more markedly in the first stage of the cycling test. In this stage and more specifically in the first 17 cycles at the end of the charge the Li_xNiO_2 compound contains only the R_2 phase, identified by Ohzuku et al. [5] as a lithium-poor NiO_2 structure. The interlayer distances in this phase is strongly reduced as revealed by the almost 1.0 Å contraction of the $\bar{c}$-parameter. This contraction is most likely related to the presence of the Ni^{4+} ions in the almost vacant 3*b* layers. Nickel atoms are present in the 3*b* layers also in highly stoichiometric samples as the presently studied with $x=0.97$ where the nickel content in the 3*b* layers is at least 0.03. Due to the high vacancy concentration at $x_{min}=0.12$ the 3*b* planes become considerably negatively charged. This can make it possible for the small Ni^{4+} ions ($r=0.55$ Å) to migrate from the 3*a* to 3*b* planes, thus additionally diminishing the interlayer distances. Such a migration has been previously indicated for cobalt in $LiCoO_2$ and of vanadium in $LiVO_2$ [11,15]. The concentrations of both nickel and vacancies in the 3*b* planes, determined by XRD and electrochemical measurements are average values and there should be some distribution among crystallites with higher and lower nickel and vacancy concentrations. The crystallites with the highest nickel and vacancy content in the 3*b* layers at the end of the charge will be partially or totally inactivated because of the strongly impeded diffusion of lithium in them. As the cycling proceeds the number of such crystallites will diminish at each charge and the capacity decay rate will be reduced. This is actually what happens when the cathode is cycled to 4.28 V in Fig. 7(c). It is quite probable that if the cycling proceeds beyond the 60th cycle and the x_{min} value is further increasing the *DR* constant would further diminish, whereby the number of cycles to the 100 mAh/g minimum could be increased. The same considerations apply also to the cathode cycled to 4.20 V, where the increase in x_{min} above 0.25 at the 16th cycle makes this process even more probable. The *DR* and capacity data derived from Fig. 7 are summarized in Fig. 8, presenting the values of DR_1 (the decay rate constant between the 1st and the 20th cycle), DR_2 (the constant from the 21st to the last cycle) and the discharge capacities at the 5th and 50th cycles as a function of x_{min} in the first cycle.

The large capacity loss of $Li_xNi_{2-x}O_2$ in the first cycle is typical for this compound and is not observed in the isostructural $LiCoO_2$ and in $LiNi_{0.5}Co_{0.5}O_2$. As seen in Fig. 7 it is constant with *n* and not affected by the increase in U_{max}. It appears that a definite amount of the vacancies generated in the first charge becomes inaccessible for lithium insertion in the next discharges, at least at a voltage close to open-circuit voltage of the uncycled, as synthesized compound, 2.60 V. In order to occupy all the vacancies after the first charge in the $Li_{0.75}\square_{0.25}NiO_2$ phase it is necessary to apply a voltage by about 1.0 V more negative, e.g. 1.75 V [2]. This strange behaviour of $Li_{0.75}\square_{0.25}NiO_2$ is apparently not related to the formation of a new phase at $x=0.75$, since the R_1 phase present in the pristine compound with $x=0.97$ is the only phase determined by XRD at the end of each discharge even after 25 cycles.

The increased diffusion resistance of lithium in $Li_{3/4}\square_{1/4}NiO_2$ could be interpreted in terms of the lithium in-plane ordering in a superlattice, where the energy to remove a lithium ion is not only a function of the lithium concentration but also of the lithium in-plane ordering, this resulting in a non-Nernstian compositional dependence of the open-circuit voltage. Such a behaviour was established by Ueda and Ohzuku [16] with the isostructural $LiNi_{0.5}Co_{0.5}O_2$ by the change in the slope of the open-circuit voltage versus *x* plot at $x=3/4$. For this composition, the authors [16] have derived a superlattice where each vacancy in the 3*b* plane is encircled by six sites occupied by lithium. Such a superstructure could impede the insertion of lithium. A similar situation could occur in the case of $Li_{0.75}\square_{0.25}NiO_2$ obtained in the first cycle.

It should be pointed our that while in $Li_{3/4}\square_{1/4}Co_{1/2}Ni_{1/2}O_2$ the lithium ordering causes only a slight change in the slope of the open-circuit voltage versus *x* plot, in the case of $Li_{0.75}\square_{0.25}NiO_2$ this leads to a drastic increase in the cathodic overpotential during the discharge to $x=1$. This makes the above interpretation a rather speculative one.

Acknowledgements

This work was supported financially in part by the National Research Fondation of Bulgaria under contract 499M/1995.

References

[1] A. Lecerf, M. Broussely and J.P. Gabano, *EP No. 0 345 707; US Patent No. 4 980 080* (1989).
[2] J.R. Dahn, U. von Sacken and C.A. Michal, *Solid State Ionics, 44* (1990) 87.
[3] W. Li and J.N. Reimers, *Phys. Rev. B, 46* (1992) 3236.
[4] J. Reimers, J.R. Dahn, J.E. Greedan, C.V. Stager, G. Lui, I. Davidson and U. von Sacken, *J. Solid State Chem., 102* (1993) 542.

[5] T. Ohzuku, A. Ueda and M. Nagayama, *J. Electrochem. Soc., 140* (1993) 1862.
[6] S. Yamada, M. Fujiwara and M. Kanda, *J. Power Sources, 54* (1995) 209.
[7] M. Broussely, F. Perton, P. Biensan, J.M. Bodet, J. Labat, A. Lecerf, C. Dalmas, A. Rougier and J.P. Peres, *J. Power Sources, 54* (1995) 109.
[8] J. Morales, C. Peres-Vincente and J. Tirado, *Mater. Res. Bull., 25* (1990) 623.
[9] R. Moshtev, P. Zlatilova and V. Manev, *Ext. Abstr., 7th Int. Meet. on Lithium Batteries, Boston, MA, USA, May 1994*, p. 492.
[10] R. Moshtev, P. Zlatilova, V. Manev and A. Sato, *J. Power Sources, 54* (1994) 329.
[11] R. Kanno, H. Kubo, Y. Kawamoto, T. Kamiyama, F. Izumi, Y. Takeda and M. Takano, *J. Solid State Chem., 110* (1994) 216.
[12] L. Xie, W. Ebner, D. Fouchard and S. Megahed, *Ext. Abstr., Electrochemical Society Meet., Miami Beach, FL, USA, Oct. 1994*, p. 162.
[13] Y. Yamaki and T. Tobishima, *Electrochim. Acta, 35* (1990) 383.
[14] W. Li, J.N. Reimers and J.R. Dahn, *Solid State Ionics, 67* (1993) 123.
[15] J.G. Goodenough, G. Dutta and A. Manthiram, *Phys. Rev. B, 43* (1991) 10170.
[16] A. Ueda and T. Ohzuku, *J. Electrochem. Soc., 141* (1994) 2010.